Available online www.worldscientificnews.com

World Scientific News

An International Scientific Journal

WSN 211 (2026) 39-51 EISSN 2392-2192

Validation of Seasonal SEIRS and Hybrid Seasonal SEIRS-Gaussian Models for Influenza Data In Indonesia

Riana N. Pakpahan [1*], Nazla Aqira Maghfirani[1], Sri Purwani[2]

[1]Master Program in Mathematics, Faculty of Mathematics and Natural Sciences, Universitas Padjadjaran, Sumedang 45363, Indonesia

[2]Department of Mathematics, Universitas Padjadjaran, Sumedang 45363 Indonesia

E-mail address: pakpahanriana97@gmail.com

ABSTRACT

Seasonal influenza in Indonesia exhibits a complex temporal pattern not fully explained by conventional seasonal models. This study develops and compares two mathematical models of its transmission dynamics: an SEIRS model with Seasonal Forcing and a Hybrid SEIRS–Gaussian Model. The models were calibrated using weekly surveillance data from WHO FluNet (June 2023–October 2025). BDS test and Recurrence Quantification Analysis (RQA) confirmed the deterministic nonlinear nature and strong seasonal pattern in the data, supporting the deterministic modeling approach. The systems of differential equations were solved numerically using the 4th-order Runge–Kutta (RK4) method, and parameter calibration was optimized with a differential evolution algorithm. Simulation results demonstrate that the Hybrid SEIRS–Gaussian Model achieves significantly greater accuracy in replicating observed data, with an RMSE of 11.847 , a Pearson correlation of 0.854, and an R^2 of 0.696, compared to the pure seasonal SEIRS model (RMSE 24.987, R^2 −0.353). These findings indicate that influenza transmission in Indonesia is not solely dependent on seasonal cycles but is also influenced by sporadic exogenous factors. Consequently, the hybrid model incorporating a Gaussian component proves more representative and reliable for analyzing and predicting influenza dynamics within the context of Indonesian tropical epidemiology.

***Keywords*:** influenza modeling, SEIRS model, seasonal forcing, Gaussian outbreak.

(Received 10 November 2025; Accepted 15 December 2025; Date of Publication 4 January 2026)

1. INTRODUCTION

Seasonal influenza remains a significant global health threat. According to the World Health Organization (WHO), annual influenza epidemics result in an estimated 3 to 5 million cases of severe illness and 290,000 to 650,000 respiratory-related deaths globally. This impact is exacerbated by the high vulnerability of specific groups, including children, the elderly, pregnant women, and individuals with chronic conditions, who consistently show higher rates of complications and mortality in epidemiological studies [1], [2], [3]. In Indonesia, influenza transmission dynamics are influenced by tropical conditions, manifesting distinct temporal patterns that can include dual-peak patterns associated with the rainy season [4]. Indonesia's national influenza surveillance system, integrated with the WHO's Global Influenza Surveillance and Response System (GISRS) network, generates weekly positive specimen data that are invaluable for monitoring trends and detecting outbreaks.

Mathematical modeling has been extensively employed to understand influenza dynamics. Previous studies include SEIR models [5], fractional-order SEIR models [6], outbreak prediction using ILI (Influenza-like Illness) data [7], and estimation of key epidemiological parameters such as the basic reproduction number R_0 using advanced statistical methods [8]. At the population level, deterministic compartment-based models such as SEIR (Susceptible-Exposed-Infectious-Recovered) and SEIRS (which accommodates temporary immunity) form the foundation of many studies due to their simplicity and ability to capture disease dynamics at a macro level [9]. To reflect the annual case fluctuations characteristic of seasonal diseases, these models are often modified by incorporating seasonal forcing, i.e., the modulation of transmission rates using periodic functions [10], [11].

Modeling approaches that integrate periodic functions into the transmission rate have long been recommended for representing annual epidemic cycles [12]. Recent research by [13] successfully integrated a Gaussian function into an SIR-SI model to represent exogenous factors in dengue cases in Peru. A similar approach has potential for adaptation to influenza, given the presence of periodic outbreak patterns not fully captured by conventional seasonal models.

Despite this progress, several research gaps remain. First, no study has yet compared mechanistic and hybrid models incorporating Gaussian components for influenza in Indonesia. Second, from a computational methodology standpoint, few journals explicitly discuss and justify the selection of the 4th-order Runge-Kutta (RK4) numerical method for solving systems with seasonal forcing and exogenous components [14].

Addressing these gaps, this study aims to: (1) develop and compare a Seasonal SEIRS model and a Seasonal SEIRS model with Gaussian Forcing, (2) implement the 4th-order Runge-Kutta (RK4) method as the numerical solver, and (3) evaluate model performance based on statistical metrics. The models will be calibrated and validated using time-series data of positive influenza specimens from WHO FluNet for Indonesia for the period June 2023–October 2025.

2. MATERIALS AND METHODS

2.1. Data Source

Influenza positive case data were obtained from WHO FluNet for the period June 1, 2023, to October 13, 2025. The data consist of the number of laboratory-confirmed positive influenza specimens reported by surveillance facilities in Indonesia.

Figure 1. WHO FluNet Surveillance Data for Seasonal Influenza Cases in Indonesia, accessed from the FluNet Chart World Health Organization (WHO) platform at: https://worldhealthorg.shinyapps.io/flunetchart/.

Figure 1. displays weekly data of positive influenza specimens in Indonesia, which show a clear seasonal pattern along with spikes in cases outside the main seasonal period. The arrows on the recurrent peaks at the end to the beginning of the year mark a consistent seasonal pattern, generally associated with the rainy season. Meanwhile, the arrows on the irregularly occurring mid-year increases indicate the presence of outbreaks that cannot be fully explained by seasonal mechanisms. These characteristics indicate that the dynamics of influenza in Indonesia are influenced not only by periodic factors but also by sporadic exogenous disturbances. This motivates the use of a hybrid model that combines seasonal forcing and a Gaussian component.

2.2. Preliminary Statistical Tests: BDS and Determinism Test

Prior to model development, we characterized the nonlinear and deterministic nature of the influenza time series using the Brock–Dechert–Scheinkman (BDS) test to detect nonlinear dependence [15], and Recurrence Quantification Analysis (RQA) to quantify the degree of determinism in the dynamical system [16].

BDS Test for Nonlinear Dependence

The BDS test examines whether a time series exhibits nonlinear dependence. The test statistic is based on the correlation integral and is defined as:

$$W_{n,m}(\varepsilon) = \sqrt{n}.\frac{\hat{C}_m(\varepsilon) - \hat{C}_1(\varepsilon)^m}{\sigma_{n,m}(\varepsilon)}$$

where is the sample size, ε is the threshold distance, and $\sigma_{n,m}$ is the standard deviation under the null hypothesis of independent and identically distributed (i.i.d.) data..

The test was applied to the residuals of an ARIMA model fitted to the influenza data. Results for embedding dimensions $m = 2,3,4$ and thresholds ε expressed in standard deviations are shown in Table 2. All p-values were below 0.05, rejecting the i.i.d. hypothesis and confirming significant nonlinear structure.

Table 1. BDS Test Results for Influenza Data Residuals

$p-value$ \ ε	5.8071	11.6141	17.4212	23.2282
$m = 2$	2e-04	0	0	0.0002
$m = 3$	0	0	2e-04	0.0020
$m = 4$	0	0	1e-04	0.0015

Recurrence Quantification Analysis (RQA)

RQA measures determinism in time series through recurrence plots. The recurrence matrix is defined as:

$$R_{i,j} = H\left(\in - \left\| x_i - x_j \right\|\right), \qquad i, j = 1,...,N$$

where H is the Heaviside function, x_i are embedded state vectors, and $\in$ is a recurrence threshold. The determinism (DET) is calculated as:

$$DET = \frac{\sum_{l=l_{\min}}^{N} lP(l)}{\sum_{i,j=1}^{N} R_{i,j}}$$

with $P(l)$ being the distribution of diagonal line lengths l.

The recurrence plot (Figure 2) showed clear diagonal patterns. Key RQA measures were: Determinism DET = 0.7075, Recurrence Rate = 0.119, Laminarity = 0.8038, Entropy = 1.5947. The high DET value (> 0.7) indicates strong deterministic dynamics, supporting the use of deterministic models.

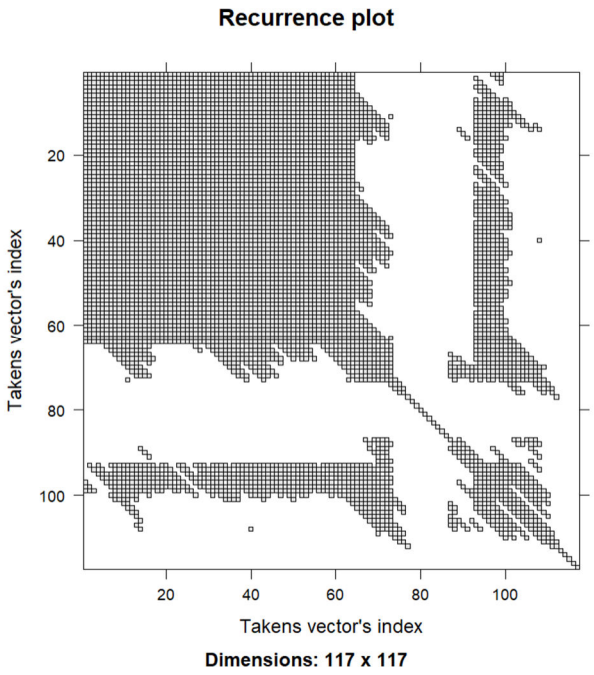

Figure 2. Recurrence plot of influenza time series (117×117).

The significant nonlinearity (BDS test) and high determinism (RQA) justify a deterministic SEIRS modeling approach augmented with non-periodic forcing to capture irregular outbreaks. These results validate the hybrid SEIRS–Gaussian structure proposed in this study.

2.3. Model

Based on the characteristic seasonal pattern observed in Indonesian influenza data, the mathematical models developed in this study are SEIRS (Susceptible-Exposed-Infectious-Recovered-Susceptible) models. The SEIRS structure was chosen due to the nature of the influenza virus, which allows recovered individuals to become susceptible again after a certain period due to waning immunity, as explained by [14].

The system of ordinary differential equations (ODEs) describing population dynamics was derived based on the S, E, I, R compartments, incorporating birth and death rates (μ), progression rate from exposed to infectious (σ), recovery rate (γ), and immunity loss rate (ω). These SEIRS equations are adopted from [17].

$$\begin{cases} \dfrac{dS}{dt} = \mu N - \dfrac{\beta(t) SI}{N} + \omega R - \mu S \\ \dfrac{dE}{dt} = \dfrac{\beta(t) SI}{N} - (\sigma + \mu) E \\ \dfrac{dI}{dt} = \sigma E - (\gamma + \mu) I \\ \dfrac{dR}{dt} = \gamma I - (\omega + \mu) R \end{cases} \quad (1)$$

where $N = S + E + I + R$ is the total population.

Model 1: SEIRS with Seasonal Forcing

To accommodate the observed seasonal pattern, the transmission rate is formulated as a periodic function of time:

$$\beta(t) = \beta_0 \left[1 + \alpha \cos\left(\frac{2\pi t}{52} + \phi \right) \right] \qquad (2)$$

where β_0 is the base transmission rate, α is the amplitude of seasonal forcing, ϕ adjusts the phase shift to align peak transmission timing, and t is time in weeks [4].

Model 2: SEIRS with Seasonal and Gaussian Forcing (Hybrid)

Indonesian influenza data show additional outbreaks beyond the regular seasonal pattern. Therefore, a Gaussian component is integrated to represent these exogenous outbreaks, adapting the approach of [13] for dengue modeling:

$$\beta(t) = \beta_0 \left[1 + \alpha \cos\left(\frac{2\pi t}{52} + \phi \right) \right] \times \left[1 + \sum_{i=1}^{k} h_i \exp\left(-\frac{(t - c_i)^2}{2w_i^2} \right) \right] \qquad (3)$$

where h_i, c_i, w_i represent the amplitude, center, and width of the i-th outbreak, respectively.

2.4. Model Parameters

Parameter values for the SEIRS model were derived from epidemiological literature, Indonesian demographic data, and calibrated against influenza surveillance data. The baseline values were selected based on established references and then refined through optimization. For the Seasonal SEIRS model, the transmission rate follows a periodic function to capture annual cycles, while the Hybrid model incorporates additional Gaussian components to represent sporadic outbreaks beyond regular seasonal patterns.

Table 2. Parameter values for the seasonally forced SEIRS model.

Parameter	Definition	Baseline Value	Source
β_0	Baseline transmission rate	0.4	Initial assumption
α	Seasonal amplitude	0.2	Initial assumption
σ	Infection progression rate	1/1,4	[14]
γ	Recovery rate	1/7	[12]
ω	Immunity loss rat	1/365	Assumed
μ	Birth/death rate	1/(70*365)	BPS Indonesia

Surveillance Scaling Factor

A surveillance scaling factor (scale) was incorporated to align simulated prevalence with observed case counts since WHO FluNet data reflect laboratory-confirmed specimens rather than true population-level incidence. The relationship is defined as:

$$\text{Reported cases } (t) = scale \times I(t)$$

The initial scale value of 0.05 assumes that a modest proportion of infections are captured by the surveillance network. This parameter was subsequently calibrated simultaneously with β₀ and α.

Gaussian Outbreak Parameters

The Hybrid SEIRS-Gaussian model extends the seasonal model by including Gaussian outbreak terms with parameters h_i (amplitude), c_i (center time), and w_i (width) that were initialized as $h_i = 0.2$, c_i at mid-series, and $w_i = 3$ weeks, then calibrated alongside β₀ and α.

2.5. Numerical Method and Calibration

The nonlinear system of ordinary differential equations incorporating seasonal and Gaussian forcing terms was solved numerically using the 4th-order Runge-Kutta (RK4) method. This explicit integrator provides a balanced compromise between accuracy and computational efficiency for stiff, time-varying dynamical systems [14]. With a weekly time step ($h = 1$ week), the RK4 update for each compartment y (i.e., S, E, I, R) is computed as:

$$y_{n+1} = y_n + \frac{1}{6}\left(k_1 + 2k_2 + 2k_3 + k_4\right)$$

where:

$$\begin{aligned} k_1 &= h \cdot f\left(t_n, y_n\right) \\ k_2 &= h \cdot f\left(t_n + \frac{h}{2}, y_n + \frac{k_1}{2}\right) \\ k_3 &= h \cdot f\left(t_n + \frac{h}{2}, y_n + \frac{k_2}{2}\right) \\ k_4 &= h \cdot f\left(t_n + h, y_n + k_3\right) \end{aligned} \tag{4}$$

where h denotes the right-hand side of the SEIRS equations (1).

Parameter calibration was carried out via the Differential Evolution (DE) algorithm [18], a population-based global optimizer well-suited to nonlinear, multi-modal objective landscapes. The algorithm was initialized with a population of $NP = 15$ candidate vectors whose components were randomly sampled within biologically plausible bounds: $\beta_0 \in [0.1, 5.0]$, $\alpha \in [0.01, 1.0]$, $\phi \in [-\pi, \pi]$, and the surveillance scaling factor $\text{scale} \in [0.001, 0.5]$.

For the hybrid model, Gaussian outbreak parameters were likewise bounded: amplitude $h_i \in [0,1]$ centers $c_i \in [0,T]$ (where T is the length of the time series in weeks), and widths $w_i \in [0,10]$ weeks.

During each generation, mutant vectors were created using the "rand/1" mutation strategy with a scaling factor $F = 0.8$, followed by binomial crossover with probability $CR = 0.7$. Selection retained the vector that yielded the lower root-mean-square error (RMSE) between simulated and observed weekly case counts:

$$RMSE = \sqrt{\frac{1}{T}\sum_{t=1}^{T}\left(I_{sim}(t) - I_{obs}(t)\right)^2}, \quad I_{sim}(t) = scale \times I_{model}(t)$$

The evolution proceeded for a maximum of $G_{\max} = 30$ generations or until convergence was detected. A final local refinement step using the L-BFGS-B algorithm ensured that the solution corresponded to a local minimum of the objective function.

2.6. Model Evaluation

Model performance was evaluated using a suite of complementary statistical metrics that assess accuracy, correlation, and goodness-of-fit [19]. The following measures were calculated for each model:
Root Mean Square Error (RMSE)

Quantifies the average magnitude of prediction errors, with lower values indicating better fit:

$$RMSE = \sqrt{\frac{1}{T}\sum_{t=1}^{T}\left(I_{sim}(t) - I_{obs}(t)\right)^2}.$$

Mean Absolute Error (MAE)

Provides a robust measure of average absolute deviation that is less sensitive to outliers than RMSE:

$$MAE = \frac{1}{T}\sum_{t=1}^{T}\left|I_{sim}(t) - I_{obs}(t)\right|.$$

Pearson Correlation Coefficient (r)

Measures the linear association between simulated and observed time series, with values near ±1 indicating strong directional agreement:

$$r = \frac{\sum_{t=1}^{T}\left(I_{sim}(t) - \bar{I}_{sim}\right)\left(I_{obs}(t) - \bar{I}_{obs}\right)}{\sqrt{\sum_{t=1}^{T}\left(I_{sim}(t) - \bar{I}_{sim}\right)^2 \sum_{t=1}^{T}\left(I_{obs}(t) - \bar{I}_{obs}\right)^2}}.$$

Coefficient of Determination (R^2)

Indicates the proportion of variance in the observed data that is explained by the model:

$$R^2 = 1 - \frac{\sum_{t=1}^{T}\left(I_{obs}(t) - I_{sim}(t)\right)^2}{\sum_{t=1}^{T}\left(I_{obs}(t) - \bar{I}_{obs}\right)^2}.$$

These metrics collectively provide a comprehensive assessment of model fidelity: RMSE and MAE quantify error magnitude, r assesses temporal alignment, and R^2 evaluates overall explanatory power.

3. RESULT AND DISCUSSION

3.1. Results

The influenza dataset used in this study was obtained from WHO FluNet from June 1, 2023, to October 13, 2025, comprising a total of 124 weekly data points and 2,685 positive influenza cases. These data represent the number of specimens collected through Indonesia's national influenza surveillance and laboratory-confirmed as positive for influenza. The specimens are reported by surveillance facilities integrated into the WHO's GISRS network. BDS and RQA test results confirmed that Indonesian influenza data are deterministic nonlinear, with a strong seasonal pattern and periodic outbreaks. The DET value of 0.7075 supports the use of deterministic models such as SEIRS.

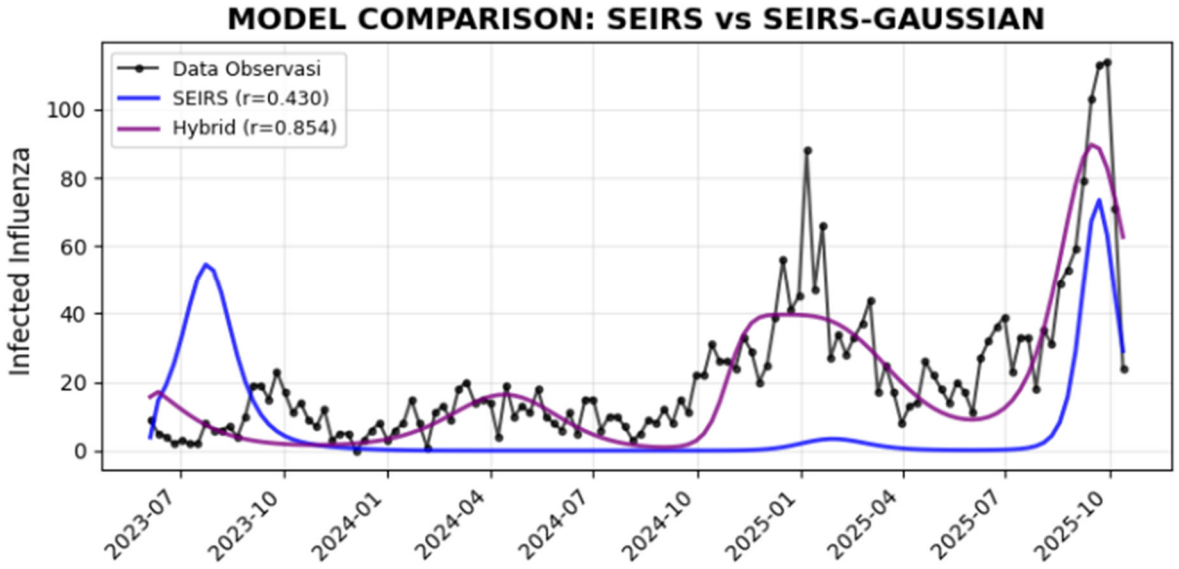

Figure 3. Comparison of SEIRS model simulation results with WHO data for Indonesia (2023–2025)

Simulation results implementing the RK4 numerical method (4), presented in Figure 3, show that the Hybrid SEIRS-Gaussian model performs significantly better in replicating the temporal pattern of observed data compared to the Seasonal SEIRS model. The hybrid model not only captures the main seasonal peaks (October–January) but also the mid-year case increases that the Seasonal SEIRS model could not produce.

The performance and calibration of both models are presented in Table 3, Table 4, and Figure 4. The Seasonal SEIRS model yielded unsatisfactory performance with an RMSE of 24.987, MAE of 20.255, and a negative R^2 (-0.353). This indicates that the conventional seasonal model is insufficient to capture the variation in Indonesian influenza data, which shows additional outbreak patterns beyond the regular seasonal cycle.

Table 3. Performance Comparison of SEIRS Models.

Model	RMSE	MAE	Correlation (r)	R^2
SEIRS Seasonal	24.987	20.255	0.430	-0.353
Hybrid SEIRS-Gaussian	11.847	8.716	0.854	0.696

Conversely, the Hybrid SEIRS-Gaussian model showed significantly better performance with an RMSE of 11.847 (52.6% lower than the baseline model), MAE of 8.716, and a Pearson correlation coefficient of 0.854. An R^2 value of 0.696 indicates that the hybrid model can explain 69.6% of the variation in the observed data.

Parameter calibration results for both models can be seen in Table 4. The differential evolution algorithm was used to minimize the Root Mean Square Error (RMSE) between simulation and observed data.

Table 4. Calibrated Parameters for the Seasonal SEIRS and Hybrid SEIRS-Gaussian Models.

Parameter	Definition	SEIRS Seasonal	Hybrid SEIRS-Gaussian	Unit
β_0	Baseline transmission rate	2.161	1.437	week^{-1}
α	Amplitude of seasonal forcing	0.400	0.146	-
ϕ	Seasonal phase shift	-2.076	-0.824	radian
Scale	Data scaling factor for specimens	0.056	0.034	-
I_0	Initial infectious individuals	18.2	15.8	individuals
E_0	Initial exposed individuals	27.3	23.7	individuals
R_0	Initial recovered individuals	9.1	7.9	individuals
h_1	Amplitude of first Gaussian	-	0.705	-
c_1	Peak position of first Gaussian	-	69.7	week
w_1	Width of first Gaussian	-	4.1	week
h_2	Amplitude of second Gaussian	-	0.755	-
c_2	Peak position of second Gaussian	-	112.9	week
w_2	Width of second Gaussian	-	10.0	week

The lower β_0 value of 1.437 in the hybrid model compared to 2.161 week^{-1} in the seasonal model indicates that the model with a Gaussian component requires a lower base transmission rate to fit the data, as additional transmission increases are provided by the Gaussian component during outbreak periods. The significant decrease in α from 0.400 to 0.146 in the hybrid model indicates that seasonal variation plays a smaller role when exogenous (Gaussian) factors are considered.

Figure 4. shows the residuals for both models. The Seasonal SEIRS model produces systematic errors with a clear residual pattern, while the hybrid model shows a more random residual distribution with smaller variance. This indicates that the hybrid model has successfully accommodated the nonlinear structure in the data.

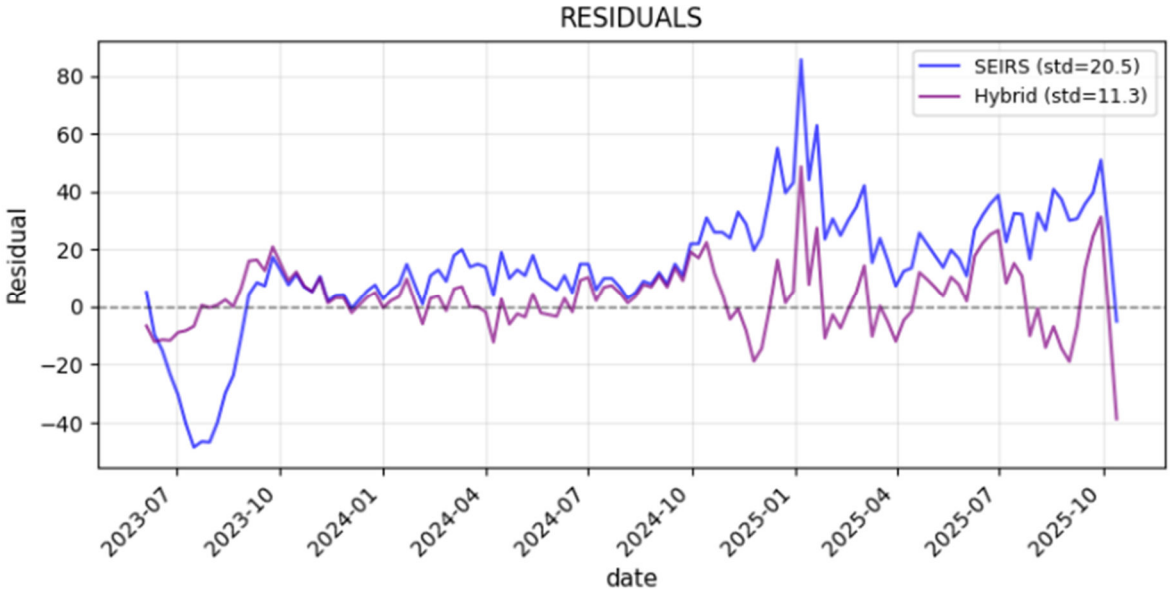

Figure 4. Residuals of the Seasonal SEIRS and Hybrid Seasonal-Gaussian SEIRS Models.

Figure 3. shows that the residual standard deviation of the Hybrid SEIRS-Gaussian Model (11.3 specimens) is significantly lower than that of the Seasonal SEIRS Model (20.5 specimens). Although the modeled data originates from specimen-based surveillance—reflecting laboratory testing capacity—this difference indicates that the hybrid model has higher consistency in replicating the temporal dynamics of surveillance data. This level of precision makes it more reliable for identifying the timing of increased influenza activity, thus potentially supporting more effective surveillance response planning and laboratory resource allocation.

3.2. Discussion

This study departs from the observation that seasonal influenza patterns in Indonesia exhibit two main characteristics: (1) regular seasonal peaks occurring around the end and beginning of the year, and (2) increased cases during periods outside the main seasonal peak. These characteristics pose a challenge for standard seasonal SEIRS models as the data pattern does not fully follow a single periodic function.

Preliminary analysis via the BDS test confirmed nonlinear dependence in the data, while the determinism value (DET = 0.7075) from RQA indicates that influenza dynamics have a strong deterministic structure. This provides a valid basis for using mechanistic SEIRS models.

Simulations using the 4th-order Runge-Kutta (RK4) numerical method were implemented due to its stability and accuracy for nonlinear systems with time-varying parameters. The key findings from the simulations are: First, the SEIRS model with seasonal forcing can capture the basic seasonal pattern but fails to represent additional outbreaks. This is evident from the high RMSE (24.987) and negative R^2 (-0.353), indicating model inadequacy for the complexity of Indonesian data. Second, the Hybrid SEIRS–Gaussian model successfully captured both types of peaks, both seasonal and those appearing sporadically.

The addition of the Gaussian component allows the model to represent exogenous disturbances affecting case increases, such as climate variability, population mobility, or viral circulation changes. This component results in a significant model performance improvement: RMSE decreased by over 50% (to 11.847), MAE decreased, and residuals were more randomly distributed. This confirms that influenza dynamics in Indonesia are a combination of seasonal and non-seasonal factors.

Parameter differences also provide insight into transmission mechanisms. The lower β_0 value in the hybrid model (1.437 vs. 2.161 week^{-1}) indicates that with the Gaussian addition, the base transmission rate need not be as high as in the pure seasonal model to explain the data. Meanwhile, the smaller seasonal amplitude α (0.146 vs. 0.400) indicates that seasonal factors still play a role, but the contribution of exogenous outbreaks is more dominant in explaining data variation.

Overall, the findings demonstrate that for tropical countries like Indonesia, seasonal representation alone is insufficient. Influenza is influenced by complex dynamics involving climatic instability, population heterogeneity, and other epidemiological factors; therefore, the hybrid model offers a more realistic approach. This model has the potential to become a more reliable tool for surveillance and public health planning. For future development, integrating more specific exogenous data, such as mobility or humidity data, could enhance the model's predictive capability.

4. CONCLUSION

This study concludes that influenza transmission dynamics in Indonesia cannot be fully explained by a model with seasonal forcing alone, as the data exhibit deterministic nonlinear patterns with case increases outside the main seasonal peak. Performance analysis proves that the Hybrid SEIRS–Gaussian Model is significantly more accurate than the Seasonal SEIRS model, with an RMSE of 11.847 (a reduction of >50%), a correlation of 0.854, and an R^2 of 0.696. These findings confirm that integrating a Gaussian component successfully represents exogenous outbreaks not captured by the seasonal function alone. Therefore, the hybrid model is more representative for the complex epidemiological context in Indonesia and has the potential to support more adaptive and data-driven surveillance policies and public health responses.

References

[1] J. García-García and C. Ramos, "[Influenza, an existing public health problem].," *Salud Publica Mex*, vol. 48, no. 3, pp. 244–67, 2006, doi: 10.1590/s0036-36342006000300009.

[2] C. Costantino and F. Vitale, "Influenza vaccination in high-risk groups: a revision of existing guidelines and rationale for an evidence-based preventive strategy.," *J Prev Med Hyg*, vol. 57, no. 1, pp. E13-8, 2016.

[3] J. Smetana, R. Chlibek, J. Shaw, M. Splino, and R. Prymula, "Influenza vaccination in the elderly.," *Hum Vaccin Immunother*, vol. 14, no. 3, pp. 540–549, Mar. 2018, doi: 10.1080/21645515.2017.1343226.

[4] J. Tamerius, M. I. Nelson, S. Z. Zhou, C. Viboud, M. A. Miller, and W. J. Alonso, "Global Influenza Seasonality: Reconciling Patterns across Temperate and Tropical Regions," *Environ Health Perspect*, vol. 119, no. 4, pp. 439–445, Apr. 2011, doi: 10.1289/ehp.1002383.

[5] F. S. Rosyada, Widowati, and S. Hariyanto, "Local stability analysis of an influenza virus transmission model case study: Tondano health center in pekalongan city," in *Journal of Physics: Conference Series*, Institute of Physics Publishing, Jun. 2019. doi: 10.1088/1742-6596/1217/1/012057.

[6] A. Daffa Akbar, "A fractional - order mathematical model of the spread of influenza," *BAREKENG: J. Math. & App*, vol. 19, no. 1, pp. 491–0502, 2025, doi: https://doi.org/10.30598/barekengvol19iss1pp0491-0502.

[7] A. Andronico, J. Paireau, and S. Cauchemez, "Integrating information from historical data into mechanistic models for influenza forecasting," *PLoS Comput Biol*, vol. 20, no. 10, Oct. 2024, doi: 10.1371/journal.pcbi.1012523.

[8] L. Y. H. Chan *et al.*, "Estimating the generation time for influenza transmission using household data in the United States," *Epidemics*, vol. 50, Mar. 2025, doi: 10.1016/j.epidem.2025.100815.

[9] H. W. Hethcote, "The Mathematics of Infectious Diseases," *SIAM Review*, vol. 42, no. 4, pp. 599–653, Jan. 2000, doi: 10.1137/S0036144500371907.

[10] L. Stone, R. Olinky, and A. Huppert, "Seasonal dynamics of recurrent epidemics," *Nature*, vol. 446, no. 7135, pp. 533–536, Mar. 2007, doi: 10.1038/nature05638.

[11] M. Imran, B. A. McKinney, A. I. K. Butt, P. Palumbo, S. Batool, and H. Aftab, "Optimal Control Strategies for Dengue and Malaria Co-Infection Disease Model," *Mathematics*, vol. 13, no. 1, p. 43, Dec. 2024, doi: 10.3390/math13010043.

[12] M. J. Keeling and P. Rohani, *Modeling Infectious Diseases in Humans and Animals*. Princeton University Press, 2011. doi: 10.2307/j.ctvcm4gk0.

[13] J. V. Bogado, D. H. Stalder, C. E. Schaerer, M. R. Soto, and D. Champin, "Temperature-based Dengue Outbreaks Modelling with Exogenous Variables," SBMAC, Dec. 2022. doi: 10.5540/03.2022.009.01.0311.

[14] J. M. Heffernan, R. J. Smith, and L. M. Wahl, "Perspectives on the basic reproductive ratio," *J R Soc Interface*, vol. 2, no. 4, pp. 281–293, Sep. 2005, doi: 10.1098/rsif.2005.0042.

[15] C. F. Baum, S. Hurn, and K. Lindsay, "The BDS test of independence," *Stata Journal*, vol. 21, no. 2, pp. 279–294, Jun. 2021, doi: 10.1177/1536867X211025796.

[16] R. Pánis, M. Kološ, and Z. Stuchlík, "Detection of chaotic behavior in time series," Dec. 2020, [Online]. Available: http://arxiv.org/abs/2012.06671

[17] O. N. Bjørnstad, K. Shea, M. Krzywinski, and N. Altman, "The SEIRS model for infectious disease dynamics," *Nat Methods*, vol. 17, no. 6, pp. 557–558, Jun. 2020, doi: 10.1038/s41592-020-0856-2.

[18] P. Virtanen *et al.*, "SciPy 1.0: fundamental algorithms for scientific computing in Python," *Nat Methods*, vol. 17, no. 3, pp. 261–272, Mar. 2020, doi: 10.1038/s41592-019-0686-2.

[19] R. J. Hyndman and A. B. Koehler, "Another look at measures of forecast accuracy," *Int J Forecast*, vol. 22, no. 4, pp. 679–688, Oct. 2006, doi: 10.1016/j.ijforecast.2006.03.001.